

# Photooxidation of Tryptophan and Tyrosine Residues in Human Serum Albumin Sensitized by Pterin: A Model for Globular Protein Photodamage in Skin

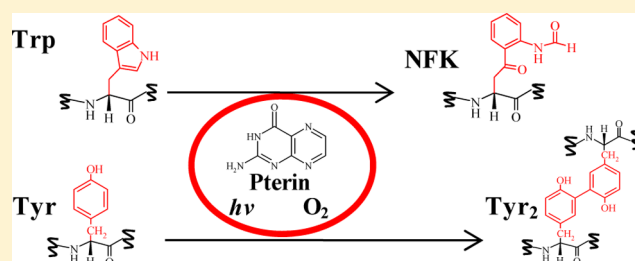
Lara O. Reid,<sup>†</sup> Ernesto A. Roman,<sup>‡</sup> Andrés H. Thomas,<sup>†</sup> and M. Laura Dántola<sup>\*,†</sup>

<sup>†</sup>Instituto de Investigaciones Fisicoquímicas Teóricas y Aplicadas (INIFTA), Departamento de Química, Facultad de Ciencias Exactas, Universidad Nacional de La Plata, CCT La Plata-CONICET, Casilla de Correo 16, Sucursal 4, 1900 La Plata, Argentina

<sup>‡</sup>Instituto de Química y Físico-Químicas Biológicas (IQUIFIB), Universidad de Buenos Aires, Junín 956, 1113 Buenos Aires, Argentina

## S Supporting Information

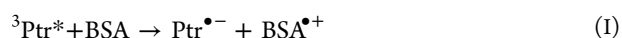
**ABSTRACT:** Human serum albumin (HSA) is the most abundant protein in the circulatory system. Oxidized albumin was identified in the skin of patients suffering from vitiligo, a depigmentation disorder in which the protection against ultraviolet (UV) radiation fails because of the lack of melanin. Oxidized pterins, efficient photosensitizers under UV-A irradiation, accumulate in the skin affected by vitiligo. In this work, we have investigated the ability of pterin (Ptr), the parent compound of oxidized pterins, to induce structural and chemical changes in HSA under UV-A irradiation. Our results showed that Ptr is able to photoinduce oxidation of the protein in at least two amino acid residues: tryptophan (Trp) and tyrosine (Tyr). HSA undergoes oligomerization, yielding protein structures whose molecular weight increases with irradiation time. The protein cross-linking, due to the formation of dimers of Tyr, does not significantly affect the secondary and tertiary structures of HSA. Trp is consumed in the photosensitized process, and *N*-formylkynurenine was identified as one of its oxidation products. The photosensitization of HSA takes place via a purely dynamic process, which involves the triplet excited state of Ptr. The results presented in this work suggest that protein photodamage mediated by endogenous photosensitizers can significantly contribute to the harmful effects of UV-A radiation on the human skin.



Pterins, a family of heterocyclic compounds, are present in biological systems in multiple forms and play different roles ranging from pigments to enzymatic cofactors for numerous redox and one-carbon transfer reactions.<sup>1,2</sup> Pterins are present in human skin, as in the case of 5,6,7,8-tetrahydrobiopterin (H<sub>4</sub>Bip), which is a cofactor for the aromatic amino acid hydroxylases<sup>3</sup> and participates in the regulation of melanin biosynthesis. Normal metabolism of H<sub>4</sub>Bip is altered in the skin of patients suffering from vitiligo,<sup>4–6</sup> a skin disorder characterized by the acquired loss of constitutional pigmentation,<sup>5</sup> and oxidized pterins accumulate in the affected tissues at concentrations that are significantly higher than those reported for healthy cells.<sup>6,7</sup> Although intracellular concentrations were not determined, it can be assumed that pterins can reach any cellular compartment because it has recently been demonstrated that pterins can freely cross phospholipid membranes.<sup>8</sup>

Under ultraviolet-A (UV-A) excitation (315–400 nm), unconjugated oxidized pterins can fluoresce, undergo photo-oxidation, and generate reactive oxygen species (ROS).<sup>9–11</sup> Several studies have demonstrated that pterin (Ptr), the parent and unsubstituted compound of oxidized pterins (Figure 1), is able to photosensitize free amino acids, such as tryptophan (Trp),<sup>12</sup> tyrosine (Tyr),<sup>13</sup> histidine (His),<sup>14</sup> peptides,<sup>15</sup> and

proteins, such as bovine serum albumin (BSA)<sup>16,17</sup> and tyrosinase.<sup>18,19</sup> In particular, the study of the photosensitization of BSA by Ptr revealed that degradation of the protein involves a type I mechanism.<sup>16</sup> The process is initiated by an electron transfer from the BSA to the triplet excited state of Ptr (<sup>3</sup>Ptr\*) (reaction I), yielding the corresponding pair of radical ions [pterin radical anion (Ptr<sup>•−</sup>) and BSA radical cation (BSA<sup>•+</sup>)]. BSA<sup>•+</sup> leads to the damage and degradation of the protein (reaction II), whereas Ptr<sup>•−</sup>, under aerobic conditions, transfers one electron to O<sub>2</sub>, regenerating Ptr and yielding superoxide anion (O<sub>2</sub><sup>•−</sup>) (reaction III), which, in turn, is converted into hydrogen peroxide (H<sub>2</sub>O<sub>2</sub>) by spontaneous disproportionation (reaction IV).<sup>16</sup> The analysis of BSA irradiated in the presence of Ptr suggested that the protein underwent cross-linking and was oxidized in at least two different and specific amino acid residues: Trp and Tyr.<sup>17</sup>



Received: May 1, 2016

Revised: August 8, 2016

Published: August 8, 2016



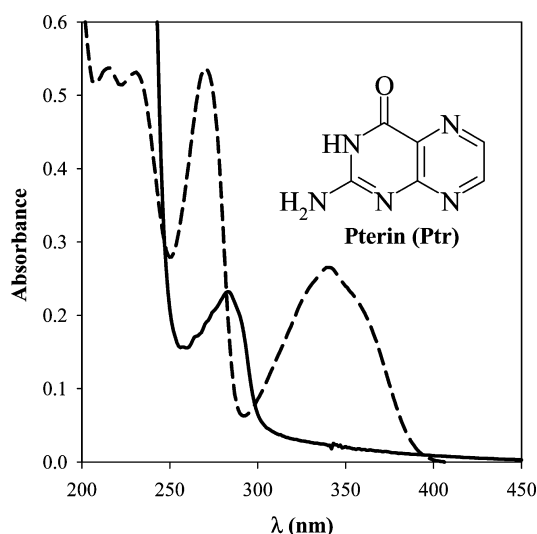
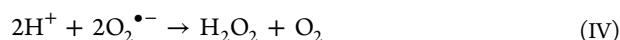


**Figure 1.** Absorption spectra in air-equilibrated aqueous solutions (pH 6.0) of Ptr (—) and HSA (---). Molecular structure of Ptr. [Ptr] = 50  $\mu$ M. [HSA] = 5  $\mu$ M. Optical path length of 1 cm.



Human serum albumin (HSA) is the most abundant protein in the circulatory system, binds and transports a wide variety of fatty acids, metabolites, and drugs.<sup>20</sup> It is a monomeric globular protein of 585 amino acid residues and contains three homologous helical domains (I–III), each containing two subdomains (A and B); its structure is stabilized by 17 disulfide bridges.<sup>21</sup> The native conformation of HSA presents two principal binding sites for aromatic and heterocyclic molecules.<sup>22</sup> HSA contains a single indole ring at Trp-214 and a particularly reactive phenolic side chain at Tyr-411.<sup>23</sup> In addition, HSA is present in human skin,<sup>24</sup> where autocrine synthesis and regulation occur.<sup>25</sup> It has been reported that in patients affected by vitiligo, epidermal albumin oxidation takes place, but the mechanism of this process has not been elucidated.<sup>26</sup>

Taking into account the fact that oxidized pterins are present in human skin under pathological conditions, in which the protection against UV radiation fails because of the lack of melanin, and the fact that HSA is one of the most abundant proteins present in skin, we principally aimed to investigate the structural and chemical changes that HSA undergoes upon UV-A exposure in the presence of Ptr and the mechanism involved. The experiments were carried out at Ptr concentrations that were on the same order of magnitude as that found in human skin affected by vitiligo.<sup>6</sup> Most of the experiments were performed at pH 6.0  $\pm$  0.1 to ensure that more than 95% of the Ptr ( $\text{pK}_a = 7.9$ )<sup>27</sup> was in the acid form, the predominant form at physiological pH (Figure 1). The photochemical reactions were followed by UV/visible spectrophotometry, fluorescence spectroscopy, sodium dodecyl sulfate–polyacrylamide gel electrophoresis (SDS–PAGE), circular dichroism, laser-flash photolysis, size exclusion chromatography coupled with spectrophotometric, fluorescence, and dynamic light scattering detection.

## MATERIALS AND METHODS

**General. Chemicals.** Pterin (Ptr, >99%) was purchased from Schircks (Jona, Switzerland) and used without further

purification. Human serum albumin (HSA, free of fatty acids and globulin), potassium iodide (KI), deuterated water ( $\text{D}_2\text{O}$ ), sodium dodecyl sulfate (SDS, ~99%), glycerol, 2-mercaptoethanol, bromophenol blue, glycine (Gly, >99% titration), ammonium persulfate (>98%), and  $N,N,N',N'$ -tetramethylethylenediamine (TEMED, ~99%) were provided by Sigma-Aldrich. Methanol was provided by Laboratorios Cicarelli. Acetic acid was provided by Anedra. Coomassie Brilliant Blue G was provided by Fluka. Acrylamide,  $N,N$ -methylene-bisacrylamide, and tris(hydroxymethyl)aminomethane (Tris) were purchased from Genbiotech. Precision Plus protein standards dual core molecular weight marker was purchased from Bio-Rad. NaCl was provided by J. T. Baker.

**Samples.** All the experiments were conducted with aqueous solutions containing Ptr, HSA, and 1 mM  $\text{K}_2\text{HPO}_4$  in the pH range of 5.9–6.1. The pH measurements were performed using a sensION+ pH31 GLP pH-meter combined with a model 5010T pH electrode (Hach) or model XC161 microelectrode (Radiometer Analytical). The pH of the aqueous solutions was adjusted by adding drops of HCl and NaOH solutions from a micropipette. The concentration of the acid and base used for this purpose ranged from 0.1 to 2 M.

**Estimation of the Concentration of HSA.** The concentration of HSA in each solution was estimated by determining the absorbance at 280 nm (before adding Ptr) and then using the Lambert–Beer law ( $A^{280} = \epsilon_{\text{HSA}}^{280} I [\text{HSA}]$ ;  $\epsilon_{\text{HSA}}^{280} = 35353 \text{ M}^{-1} \text{ cm}^{-1}$ ;<sup>28</sup>  $I$  is the optical path length).

**Steady State Irradiation.** The continuous irradiation of the solutions containing Ptr and HSA was conducted via irradiation in quartz cells (0.4 cm optical path length) at different temperatures using a temperature controller (LFI-3751, Wavelength Electronics). Two radiation sources were employed: (I) Rayonet RPR 3500 lamps (Southern N.E. Ultraviolet Co.) with emission centered at 350 nm [bandwidth (full width at half-maximum) of ~20 nm] and (II) a 450 W Xe lamp with a Horiba-Jobin-Yvon model FL-1004 monochromator (single-grating spectrometer, 330 nm blaze grating). Photolysis experiments were performed in air-equilibrated aqueous solutions.

The incident photon flux densities ( $q_{\text{np}}^{0,\text{V}}$ ) at the excitation wavelength, which is the number of incident photons per time interval divided by the volume of the sample,<sup>29</sup> were  $(2.5 \pm 0.2) \times 10^{-5}$  and  $(6.7 \pm 0.6) \times 10^{-6} \text{ einstein L}^{-1} \text{ s}^{-1}$  for radiation sources I and II, respectively. The method for the determination of  $q_{\text{np}}^{0,\text{V}}$  has been described in detail previously.<sup>30</sup>

**Analysis of Irradiated Solutions. UV/Vis Analysis.** Electronic absorption spectra were recorded on a Shimadzu UV-1800 spectrophotometer. Measurements were made using quartz cells with an optical path length of 0.4 or 1 cm. The absorption spectra of the solutions were recorded at regular intervals of irradiation time.

**Liquid Chromatography (LC). High-Performance Liquid Chromatography (HPLC).** Prominence equipment from Shimadzu [solvent delivery module LC-20AT, on-line degasser DGU-20A5, communications bus module CBM-20, auto sampler SIL-20A HT, column oven CTO-10AS VP, photodiode array (PDA) detector SPD-M20A, and fluorescence (FL) detector RF-20A] was employed for monitoring the photochemical processes. A BioSep-SEC-s2000 column (silica, 300 mm  $\times$  7.8 mm, 14.5  $\mu$ m, Phenomenex) was used for product separation. Twenty millimolar Tris-HCl and 50 mM NaCl (pH 7.0) were used as the mobile phase. In some cases, for further analysis, different fractions were isolated from HPLC runs

(preparative HPLC) by collecting the mobile phase after it had passed through the PDA detector. In this case, H<sub>2</sub>O and 50 mM NaCl (pH 7.0) were used as the mobile phase.

**Fast Performance Liquid Chromatography (FPLC).** FPLC equipment coupled with an UV (Jasco UV 2075plus) and a Mini Dawn static light scattering (LS) detector (Wyatt), both coupled to a Superdex S-200 HR 10/30 column (Pharmacia Biotech), was used. The column was equilibrated with a buffer that consisted of 20 mM Tris-HCl and 100 mM NaCl (pH 7.0) as the mobile phase. In the LS detector, the scattered light was collected at three different angles and the molar mass was obtained using ASTRA Software. The scattered light at 90° was directed through an optical fiber to a Quasi Elastic Light Scattering module (Wyatt). Here, the time-dependent fluctuations in the intensity of the scattered light were registered and quantified via a second-order correlation function, and the diffusion coefficient was obtained.

**Fluorescence Spectroscopy.** Fluorescence measurements were performed using model FL3 TCSPC-SP single-photon-counting equipment (Horiba Jobin Yvon). The equipment has been previously described in detail.<sup>31</sup> Briefly, the sample solution in a quartz cell was irradiated with a 450 W xenon source through an excitation monochromator. The fluorescence, after passing through an emission monochromator, was registered at 90° with respect to the incident beam using a room-temperature R928P detector. The emission measurements were performed at 25 °C, using the temperature controller mentioned above. Corrected fluorescence spectra obtained by excitation at 295, 310, and 360 nm were recorded in the ranges of 300–500, 330–550, and 385–550 nm, respectively.

**Electrophoretic Analysis.** Protein damage was evaluated by SDS–PAGE. Samples of protein solutions were boiled for 5 min in a 0.06 M Tris-HCl (pH 6.8) solution containing 2% SDS, 10% glycerol, 1% 2-mercaptoethanol (as a reducing agent), and 0.02% bromophenol blue (as a tracking dye). Acrylamide (4%) stacking gel, 10% acrylamide resolving gel, and running buffer containing 25 mM Tris, 192 mM Gly, and 0.1% SDS (pH 8.3) were used. Electrophoresis was performed at 30 mA for 60 min. Gels were stained with 0.1% Coomassie Brilliant Blue G and destained with a solution of methanol and acetic acid for 1 h. The electrophoretic bands were quantified by scanning photodensitometry using ImageJ version 1.45s.

**Circular Dichroism Spectroscopy (CD).** Ellipticity ( $\theta$ ) of protein samples was evaluated using a Jasco model 810 spectropolarimeter calibrated with (+)-10-camphorsulfonic acid. Far- and near-UV CD spectra were recorded in the ranges between 200 and 250 nm and between 250 and 320 nm, respectively. The protein concentration was 45  $\mu$ M, and a cell with a path length of 0.1 cm was used for far-UV measurements. For near-UV CD spectra, the path length of the cell was 1.0 cm. In all cases, data were acquired at a scan speed of 20 nm min<sup>−1</sup> and at least three scans were averaged for each sample. Blank scans were subtracted from the spectra, and molar ellipticity values ( $[\theta]$ ) were expressed in units of degrees square centimeter per decimole.

**Transient Absorption Experiments.** Laser-flash photolysis (LFP) experiments were performed using a homemade laser-flash photolysis system. Ptr excitation was performed with the third harmonic at 355 nm of a Nd:YAG Minilite II laser (5 mJ per pulse, 7 ns full width at half-maximum) of Continuum. The laser beam was directed at a right angle to the analyzing beam from a xenon arc lamp (Luzchem, Cermex, US)

synchronized with a controlled shutter (Uniblitz, Vincent Associates, Rochester, NY). The detection system comprises a monochromator (model 101, Photon Technology International, Lawrenceville, NJ) and a red extended photomultiplier (model R928, Hamamatsu Photonics). The transient signals of an air-equilibrated aqueous solution of Ptr (120  $\mu$ M) were acquired with a Tektronix TDS3032B 300 MHz instrument, and up to 30 single-shot signals were averaged. Decays at 300 nm were analyzed using Origin Microcal version 8.5 with a single-exponential function to obtain the Ptr triplet excited state lifetime ( $\tau_T$ ).

## RESULTS AND DISCUSSION

**Photo-Cross-Linking of HSA.** To evaluate the capability of Ptr to photoinduce damage of human serum albumin (HSA), aqueous solutions of the protein were exposed to UV-A radiation (350 nm, radiation source I) in the presence of Ptr. The electrophoretic analysis (SDS–PAGE, [Materials and Methods](#)) of the treated samples showed a decrease in the HSA concentration as a function of irradiation time ([Figure 2](#)).

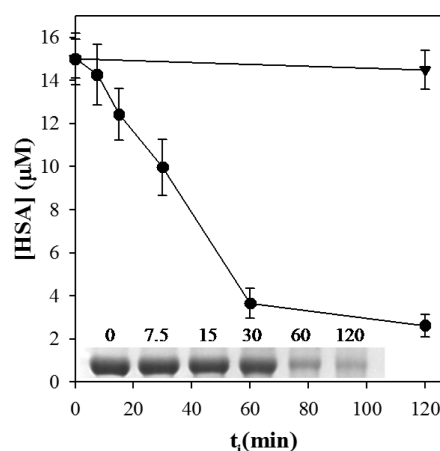


**Figure 2.** Evolution of the HSA concentration, estimated by SDS–PAGE, of an aqueous solution of HSA in the absence ( $\blacktriangledown$ ) and presence ( $\bullet$ ) of Ptr as a function of irradiation time ( $t_i$ ). The inset shows the electrophoretic bands of HSA irradiated in the presence of Ptr. The irradiation time (minutes) appears above each band. [HSA] = 15  $\mu$ M. [Ptr] = 45  $\mu$ M. [K<sub>2</sub>HPO<sub>4</sub>] = 1 mM. pH = 6.0.

No changes in HSA were detected by SDS–PAGE analyses in solutions containing both compounds at different concentrations kept in the dark for more than 3 h. Therefore, thermal reaction mixtures with Ptr and HSA were discarded. In another set of control experiments, HSA solutions were irradiated in the absence of Ptr and no chemical modification of the protein was detected, even after irradiation for more than 2 h ([Figure 2](#)). Consequently, as expected, direct effects of the radiation on the HSA molecule can be dismissed. These results suggested that the consumption of HSA could be attributed to the photosensitized process performed by Ptr.

The chromatographic analysis of the irradiated samples using the FPLC–LS system ([Materials and Methods](#)) showed that the intensity of the peak corresponding to HSA decreased as a function of irradiation time, whereas many products appeared at lower retention times ( $t_R$ ) ([Figure 3](#)). Because a size exclusion column was used, these results indicated that the molecular weights of the photoproducts were higher than that of the HSA. This behavior allows us to infer that the decrease in



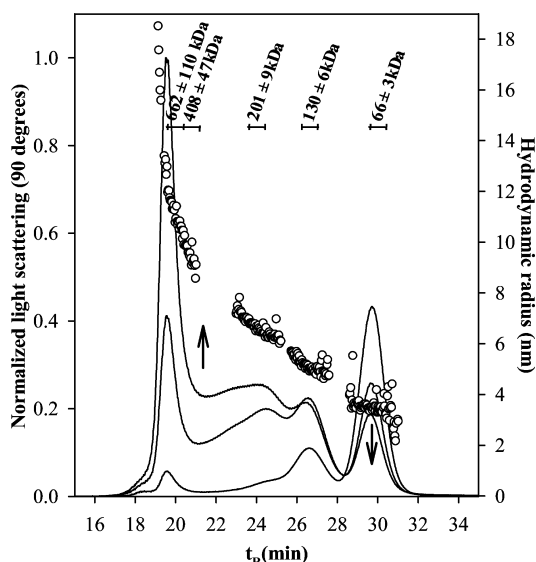


**Figure 3.** Chromatograms obtained using FPLC–LS analysis of a solution of HSA irradiated in the presence of Ptr for different amounts of time (0, 1, and 2 h). Circles represent the hydrodynamic radii of the molecules present in the sample after irradiation for 2 h. The corresponding molecular masses at different retention times are indicated in the top part of the figure. [HSA] = 100  $\mu$ M. [Ptr] = 90  $\mu$ M. [K<sub>2</sub>HPO<sub>4</sub>] = 1 mM. pH = 6.0.

the intensity of the electrophoretic band of HSA in irradiated solutions (Figure 2) is due to the formation of larger products.

In the case of BSA, it was demonstrated that dimers of the protein were produced by photosensitization with Ptr,<sup>17</sup> but larger products were not investigated. For HSA, we determined the molecular weight of the photoproducts over a broader range by analyzing the scattering profiles obtained for different irradiation times. Before irradiation, the main peak of scattered light corresponded to a species with a molecular weight of  $66 \pm 3$  kDa, which is the value reported for HSA (Figure 3). The chromatogram of the solution irradiated for 60 min showed a large peak with a molecular weight of  $130 \pm 6$  kDa, indicating formation of dimers of HSA. However, the concentration of these dimeric photoproducts did not increase steadily with irradiation time. In contrast, the sample irradiated for 120 min showed a lower concentration of dimers (Figure 3). This fact is logical taking into account that products with a higher molecular weight were detected and their concentration increased with irradiation time. Moreover, products with a molecular weight corresponding to more than 10 molecules of HSA were registered (Figure 3).

To obtain further information about the high-molecular weight photoproducts, the hydrodynamic radii ( $R_H$ ) of the compounds with different  $t_R$  values were calculated (Figure 3). FPLC analysis demonstrated that the photosensitization by Ptr leads to protein cross-linking and that such a process is not just a dimerization, as it was proposed for BSA. Instead, it is a photoinduced oligomerization that yields large protein structures with more than 10 HSA molecules and intermediate species.

**Investigation of Dimers of Tyrosine.** Covalent cross-linking mediated by disulfide bridges, histidine–lysine linkages, and tyrosine dimers (denoted Tyr<sub>2</sub>) contribute to the oxidative modification of proteins.<sup>32</sup> Because protein oxidation is increasingly being identified as a pathological manifestation, interest in cross-linking has also grown in recent years. It is

known that, under UV-A irradiation, Ptr is able to produce the dimerization of free Tyr.<sup>13</sup> The dimerization, via deformation of Tyr<sub>2</sub>, of  $\alpha$ -melanocyte-stimulating hormone ( $\alpha$ -MSH), a peptide that stimulates the production and release of melanin by melanocytes in skin and hair,<sup>15</sup> and BSA by Ptr, has also been reported.<sup>17</sup> To investigate if Tyr<sub>2</sub> is formed during the photosensitization of HSA by Ptr, fluorescence experiments were performed, taking advantage of its particular emission features. The absorption and emission spectra of Tyr<sub>2</sub> are red-shifted with respect to those of Tyr.<sup>33</sup>

Therefore, the emission spectra under excitation at 310 nm were registered for irradiated solutions of Ptr and HSA (radiation source I). The spectrum registered for each irradiation time was corrected by subtracting the spectrum of the solution before irradiation, which represents the fluorescence of Ptr (a broad emission band centered at 439 nm).<sup>11</sup> Results showed an emission band with a maximum compatible with that expected for Tyr<sub>2</sub>,<sup>33</sup> and that the intensity of this emission increased as a function of irradiation time (Figure 4).

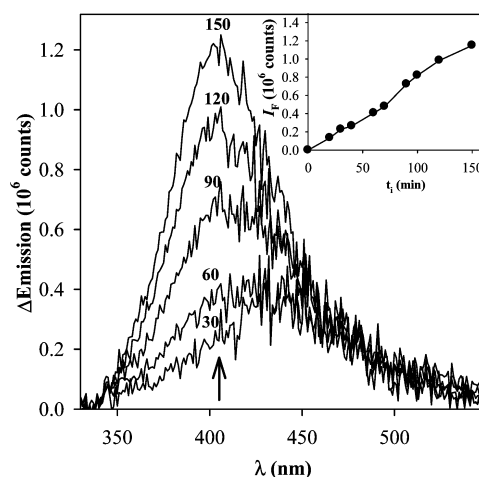


**Figure 4.** Corrected fluorescence spectra ( $\lambda_{\text{exc}} = 310$  nm) of an aqueous solution of HSA irradiated in the presence of Ptr. The irradiation time (minutes) appears above each spectrum. For each time, the spectrum of the solution before irradiation was subtracted. The inset shows the increase in fluorescence intensity ( $I_F$ ) at 405 nm as a function of irradiation time. [HSA] = 15  $\mu$ M. [Ptr] = 15  $\mu$ M. [K<sub>2</sub>HPO<sub>4</sub>] = 1 mM. pH = 6.0.

The results of analysis using HPLC–PDA (Materials and Methods) were in agreement with the results of FPLC–LS analysis, i.e. products with higher molecular weight than HSA were formed as a function of irradiation time (Figure 5). On the other hand, the intensity of the peak corresponding to Ptr did not decrease upon irradiation, indicating that the sensitizer is not consumed during the photosensitization process (Figure 5). This equipment, coupled to a fluorescence detector (HPLC–FL), was used to analyze the emission properties of the products. Figure 5 shows that the products larger than HSA fluoresce at 405 nm upon excitation at 310 nm, which agrees with the results of the fluorescence experiments presented in Figure 4.

The HPLC–PDA equipment was used to isolate the monomer (monomer fraction), the higher-molecular weight products (oligomer fraction), and the total protein (protein fraction) (Materials and Methods and Figure 5). Fluorescence analysis of these fractions allowed us to investigate the emission

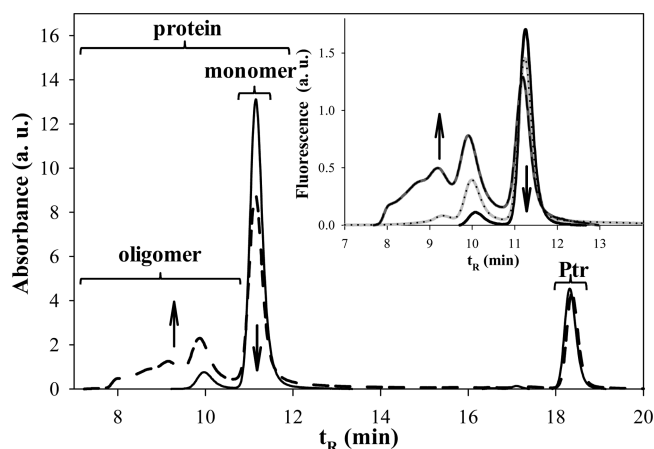


**Figure 5.** Chromatograms, obtained using the HPLC–PDA system at 280 nm, of a solution containing HSA and Ptr before (—) and after (---) irradiation for 150 min. The different fractions isolated for further studies are indicated above the corresponding peaks. The inset shows the chromatograms obtained in HPLC–FL analysis ( $\lambda_{\text{exc}} = 310$  nm;  $\lambda_{\text{em}} = 405$  nm) of HSA before and after irradiation for 90 and 150 min in the presence of Ptr. [Ptr] = 15  $\mu\text{M}$ . [HSA] = 15  $\mu\text{M}$ . [ $\text{K}_2\text{HPO}_4$ ] = 1 mM. pH = 6.0.

properties of the photoproducts without the interference of the emission of the photosensitizer.

Oxidation products of Trp (*vide infra*) present emission properties similar to those of Tyr<sub>2</sub>. However, Tyr<sub>2</sub> has a characteristic acid–base equilibrium (Figure 6) that provides emission properties that depend on the pH that can be used to identify it. The alkaline form of Tyr<sub>2</sub> exhibits an absorption band centered at 316 nm, which is not present in the

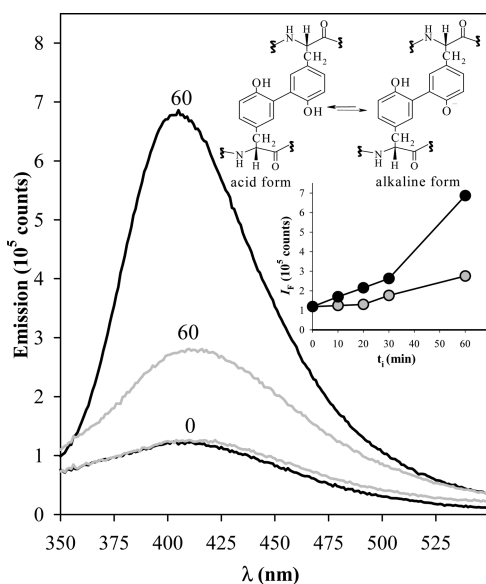


**Figure 6.** Corrected fluorescence spectra ( $\lambda_{\text{exc}} = 310$  nm) of the oligomer fraction [preparative HPLC (Figure 5)] of irradiated solutions at pH 4.5 (gray line) and pH 8.5 (black line). The irradiation time (minutes) appears above each spectrum. The inset shows a comparison of the increase in fluorescence intensity ( $I_F$ ) at 405 nm of the oligomer fraction as a function of irradiation time, at pH 4.5 (gray circles) and pH 8.5 (black circles). Acid–base equilibrium in an aqueous solution of Tyr<sub>2</sub>. [Ptr] = 15  $\mu\text{M}$ . [HSA] = 15  $\mu\text{M}$ . [ $\text{K}_2\text{HPO}_4$ ] = 1 mM. pH = 6.0.

absorption spectrum of the corresponding acid form.<sup>34</sup> Excitation at a wavelength corresponding to that energy band leads to the typical emission spectrum centered at  $\sim 405$  nm. Therefore, we expect that at pH <6, Tyr<sub>2</sub> will not emit. The oligomer fraction (Figure 5) of solutions of HSA irradiated in the presence of Ptr (radiation source I) for different times was isolated from the HPLC runs, and emission spectra were recorded at two pH values (4.5 and 8.5) (Figure 6). At alkaline pH, an emission band with a maximum coinciding with that expected for Tyr<sub>2</sub><sup>34</sup> was registered and its intensity increased as a function of irradiation time (Figure 6). In addition, the fluorescence intensity decreased significantly when the pH decreased (Figure 6). This result confirmed that Tyr<sub>2</sub> was formed when an aqueous solution of HSA was exposed to UV–A radiation in the presence of Ptr. It is worth mentioning that the samples at acidic pH showed a residual emission with a slightly red-shifted maximum in comparison with that of the sample at alkaline pH, thus suggesting that Tyr<sub>2</sub> was not the only product responsible for the emission of the oligomer fraction.

In some proteins, in particular globular ones, cross-linking of Tyr residues could lead to alteration of the conformation and biological activity.<sup>32</sup> To determine if Tyr linkages of HSA photoinduced by Ptr produce modification of the tertiary and secondary structures of HSA, aqueous solutions of HSA were irradiated in the presence of Ptr (radiation source I) during different periods of time, and the far- and near-UV CD spectra were acquired. The results (Figure 7) showed that CD spectral features are not significantly altered upon irradiation, indicating that there are no major changes in protein conformation upon Tyr photo-cross-linking.

**Photochemical Modification of the Trp Residue.** In proteins, Trp and Tyr residues act as intrinsic fluorescence probes. When an excitation wavelength of 295 nm is used, only the Trp residue is excited. Therefore, to study the effect of the photochemical process on the Trp residue, emission spectra under excitation at 295 nm of solutions containing Ptr and HSA were registered for various irradiation times. Under these conditions, fluorescence spectra presented two bands with emission maxima at 346 and 437 nm, corresponding to HSA and Ptr, respectively (Figure S1). Upon irradiation, the intensity of the HSA band decreased as a function of time, indicating the modification of the Trp residue, whereas the Ptr band remained unchanged (Figure S1), which is in agreement with HPLC analysis (Figure 5). No changes in the total fluorescence intensity of the aqueous solution of HSA in the absence of Ptr were detected, even after irradiation for more than 120 min, thus excluding the possibility that spurious effects of direct light absorption by the protein could affect its fluorescence (Figure S1).

To prevent the contribution of the fluorescence of Ptr, the protein fraction (Figure 5) of each irradiated sample was isolated from the HPLC runs, and a strong decrease in Trp emission was observed as a function of irradiation time (Figure 8). The tryptophan fluorescence features are affected by the polarity of its surrounding environment.<sup>35</sup> When a Trp residue in an apolar environment, as in the case of HSA, becomes hydrogen bonded or exposed to water, the emission shifts to longer wavelengths and its fluorescence quantum yield ( $\Phi_F$ ) decreases. In our system, the emission maximum did not change with irradiation time (Figure S1 and Figure 8), suggesting that the decrease in emission is mainly due to a

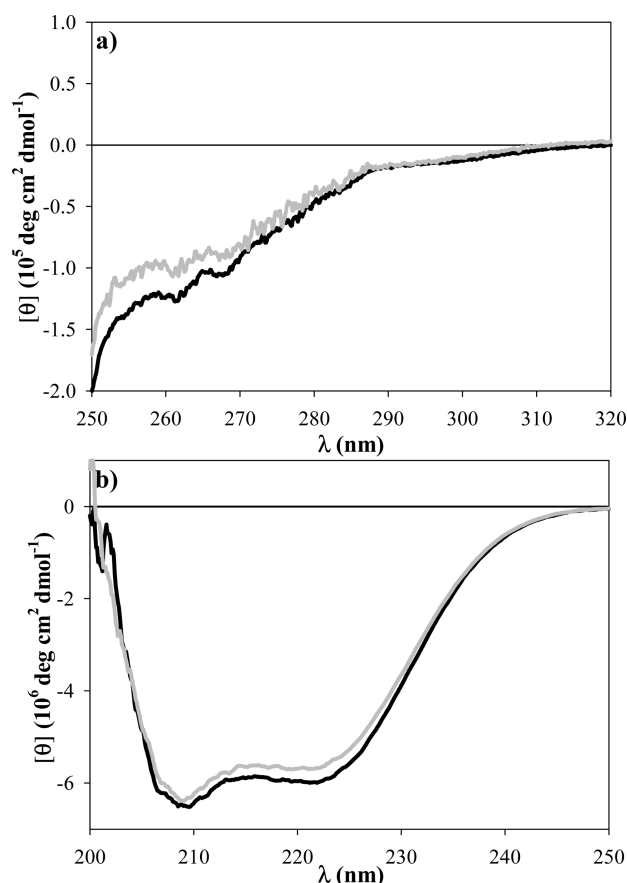


**Figure 7.** Time evolution of the (a) near-UV CD and (b) far-UV CD spectra of an air-equilibrated aqueous solution of HSA irradiated in the presence of Ptr. Spectra were recorded before (black line) and after (gray line) irradiation for 120 min. [Ptr] = 35  $\mu$ M. [HSA] = 45  $\mu$ M. [K<sub>2</sub>HPO<sub>4</sub>] = 1 mM. pH = 6.0.

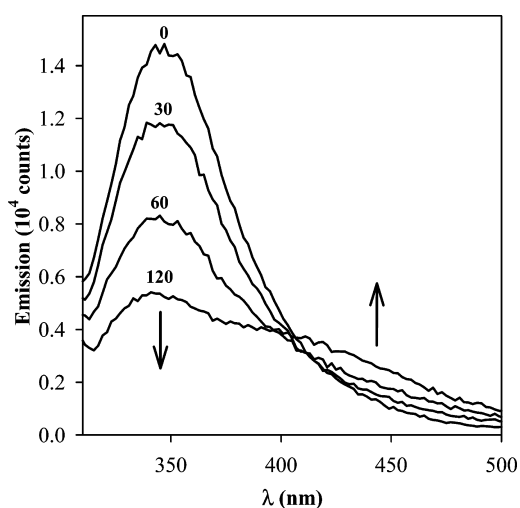


**Figure 8.** Corrected fluorescence spectra ( $\lambda_{\text{exc}} = 295$  nm) of the protein fraction (pH 7.0), isolated (preparative HPLC) from an irradiated solution containing HSA (15.0  $\mu$ M), Ptr (45.0  $\mu$ M), and K<sub>2</sub>HPO<sub>4</sub> (1 mM, pH 6.0). Irradiation times appear above each spectrum.

net consumption of Trp residues, and changes in the environment are negligible.

Besides the expected decrease in the fluorescence of Trp, an increase in the emission of the samples above 400 nm was observed (Figure 8). It is well-known that some products of the oxidation of Trp are also fluorescent with emission bands in the visible region. In addition, it has been reported that the oxidation of free Trp photosensitized by Ptr generates the typical oxidation product *N*-formylkynurenine (NFK),<sup>12</sup> which has characteristic fluorescence properties; e.g., its emission spectra, obtained by excitation of the low-energy band, consist of a broad fluorescence band centered at 435 nm.<sup>36</sup> Therefore, the fluorescence of both Tyr<sub>2</sub> and oxidation products of Trp might contribute to the emission of the irradiated samples observed in the visible region (Figure 8). To eliminate the emission of Tyr<sub>2</sub>, the protein fractions were acidified to pH 4.5 and the corresponding emission spectra by excitation at 360 nm, where the acid form of Tyr<sub>2</sub> does not absorb, were recorded. The results (Figure 9) showed emission spectra

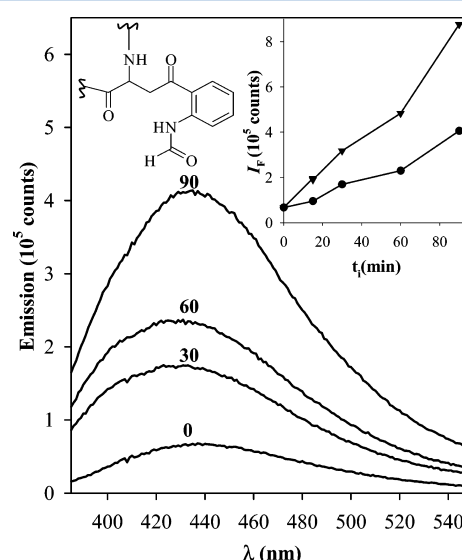


**Figure 9.** Corrected fluorescence spectra ( $\lambda_{\text{exc}} = 360$  nm) of the protein fraction (pH 4.5), isolated (preparative HPLC) from a solution containing HSA (15.0  $\mu$ M), Ptr (45.0  $\mu$ M), and K<sub>2</sub>HPO<sub>4</sub> (1 mM, pH 6.0) after irradiation for 0, 30, 60, and 90 min. The inset shows the evolution of the fluorescence intensity ( $I_F$ ) of the Trp residue in irradiated H<sub>2</sub>O (●) and D<sub>2</sub>O (▼) solutions of HSA and Ptr (pH/pD 6.0). The chemical structure of NFK is also shown.

identical to that reported for NFK,<sup>36</sup> whose intensity increased with irradiation time; this confirmed the formation of this oxidation product during the irradiation of HSA in the presence of Ptr. To the best of our knowledge, these results showed for the first time that NFK is produced in HSA by the photosensitized oxidation of the Trp residue.

**Mechanistic Aspects.** Association with a protein can modify the properties of a photosensitizer and, as a result, the efficiency and the mechanism of the photodamage to the macromolecule. This fact can be particularly important for albumins because of their high physiological concentrations and binding capacity.<sup>37</sup> In a recent work, we have demonstrated that BSA is able to bind Ptr, but the corresponding binding constant, compared to those reported for other photosensitizers, reveals that the affinity of BSA for Ptr is relatively low.<sup>16</sup> Consequently, we set out to investigate, by means of fluorescence measurements, if the interaction between HSA and Ptr is significant under our experimental conditions.

Emission spectra of Ptr were recorded between 370 and 550 nm at 25 °C in the presence of increasing concentrations of the protein. The fluorescence intensity of Ptr remained constant in the range of concentrations used in the photosensitization experiments (0–100  $\mu\text{M}$ ), thus suggesting that HSA does not bind Ptr under our experimental conditions.

Considering the discussion in the previous paragraph, a contribution of a static mechanism, initiated by Ptr associated with the protein, seems unlikely, and a purely dynamic process can be assumed. To investigate this point, irradiation experiments (radiation source II) were performed at various temperatures. A higher temperature results in faster diffusion and hence a higher level of molecular collision. Therefore, if a dynamic mechanism is responsible for the photosensitization, we should observe faster protein damage when the temperature increases. In contrast, if the reaction involves associated molecules, a high temperature tends to disrupt the ground state complex, and consequently, a decrease in the rate of photosensitized process with an increase in temperature should be observed. As expected, under our experimental conditions, it was observed that the rate of Trp consumption, estimated from the evolution of its fluorescence intensity, increased with temperature (Figure 10), thus confirming that the photo-damage to the Trp residue of HSA by Ptr takes place via a purely dynamic mechanism.

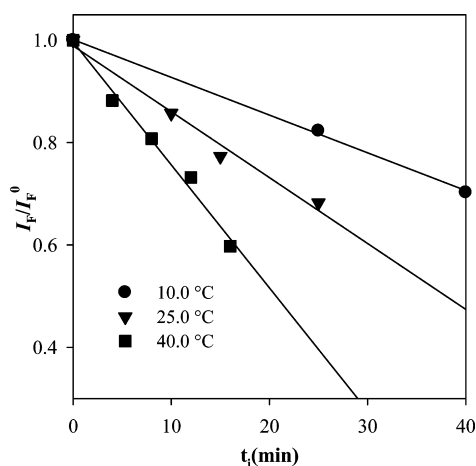


**Figure 10.** Evolution of the relative total fluorescence intensity ( $I_F/I_F^0$ ) of an aqueous solution of HSA and Ptr as a function of irradiation time (minutes) at various irradiation temperatures. Irradiation was performed at 350 nm (radiation source II). Emission spectra were recorded at 25 °C by excitation at 295 nm. [Ptr] = 45  $\mu\text{M}$ . [HSA] = 15  $\mu\text{M}$ . [ $\text{K}_2\text{HPO}_4$ ] = 1 mM. pH = 6.0.

UV-A irradiation of Ptr produces a singlet excited state ( $^1\text{Ptr}^*$ )<sup>38</sup> and a long-lived triplet excited state ( $^3\text{Ptr}^*$ ),<sup>39</sup> the latter being responsible for the photosensitized reactions using nucleotides,<sup>40,41</sup> amino acids,<sup>12–14</sup> and proteins<sup>16–19</sup> as targets. Therefore, to confirm that the photosensitized damage to HSA is initiated by  $^3\text{Ptr}^*$ , irradiation experiments were performed in the presence of iodide ( $\text{I}^-$ ), which is a selective quencher of  $^3\text{Ptr}^*$  in the concentration range of 100–300  $\mu\text{M}$ .<sup>42,43</sup> SDS-PAGE analysis of irradiated solutions showed that the rate of HSA degradation was lower in the presence of  $\text{I}^-$  than in its absence (Figure 11). The same behavior was observed when we analyzed the damage in the Trp residue of HSA by fluorescence spectroscopy (data not shown).

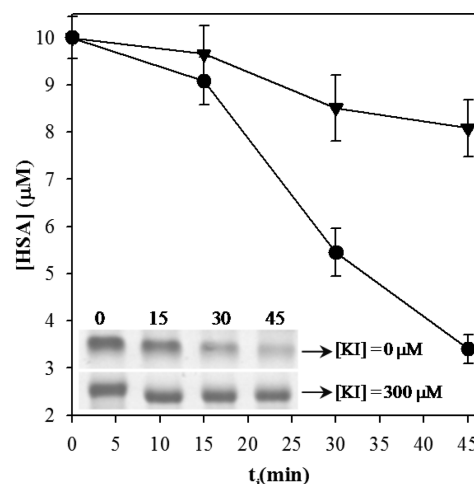


**Figure 11.** Evolution of HSA concentration, estimated by means of SDS-PAGE, as a function of irradiation time in an air-equilibrated aqueous solution of HSA and Ptr, in the presence ( $\blacktriangledown$ ) and absence ( $\bullet$ ) of KI. The inset shows the electrophoretic bands of HSA. The irradiation time (minutes) appears above each band. [HSA] = 10  $\mu\text{M}$ . [Ptr] = 100  $\mu\text{M}$ . [KI] = 300  $\mu\text{M}$ . [ $\text{K}_2\text{HPO}_4$ ] = 1 mM. pH = 6.0.

In addition, the interaction between  $^3\text{Ptr}^*$  and the protein was investigated by LFP experiments, under aerobic conditions. The rate constant of quenching of  $^3\text{Ptr}^*$  by HSA ( $k_q^{\text{HSA}}$ ) was calculated using the Stern–Volmer equation (eq 1):

$$\frac{\tau_T^0}{\tau_T} = 1 + \tau_T^0 k_q^{\text{HSA}} [\text{HSA}] \quad (1)$$

where  $\tau_T^0$  and  $\tau_T$  are the lifetimes of  $^3\text{Ptr}^*$  in the absence and presence of HSA, respectively. The  $\tau_T$  values were calculated from the corresponding decays (Figure 12) for different HSA concentrations ( $\tau_T^0 = 1.5 \mu\text{s}$ ); the Stern–Volmer plot obtained (Figure 12) was linear, and a  $k_q^{\text{HSA}}$  value of  $(4.5 \pm 0.7) \times 10^9 \text{ M}^{-1} \text{ s}^{-1}$  was determined. Hence, these results confirm the efficient quenching of  $^3\text{Ptr}^*$  by HSA.

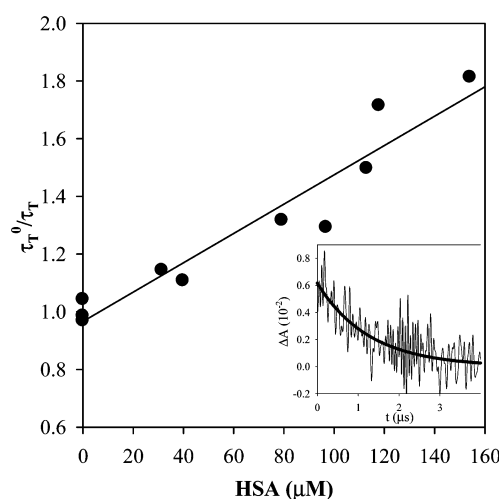


**Figure 12.** Stern–Volmer plot of the quenching of  $^3\text{Ptr}^*$  by HSA.  $\tau_T$  values were calculated by analyzing the transient absorbance  $\Delta A$  vs  $t$ . The excitation wavelength was 355 nm, the analysis wavelength 300 nm, and the Ptr concentration 120  $\mu\text{M}$ . The inset shows the time dependence of the absorbance at 300 nm, with monoexponential fitting analysis.



Results analyzed so far indicate that the photosensitization of HSA is a purely dynamic process initiated by  $^3\text{Ptr}^*$ . In general, it is accepted that the photosensitization of proteins occurs mainly through oxidation by singlet oxygen ( $^1\text{O}_2$ ), produced by the transfer of energy from the triplet excited state of the photosensitizer to the dissolved oxygen (mechanism type II).<sup>44</sup> However, results of LFP experiments presented in the previous paragraph, in agreement with a recent work on photosensitization of BSA,<sup>16</sup> suggested that transfer of an electron (mechanism type I) from the protein to  $^3\text{Ptr}^*$  may also be involved. Moreover, the formation of Tyr<sub>2</sub> has been reported as a typical product of the type I mechanism.<sup>45,46</sup> Therefore, to evaluate the contribution of oxidation by  $^1\text{O}_2$ , comparative experiments using H<sub>2</sub>O and D<sub>2</sub>O as solvents were conducted. Given that the  $^1\text{O}_2$  lifetime ( $\tau_\Delta$ ) in D<sub>2</sub>O is longer than that in H<sub>2</sub>O by a factor of approximately 15,<sup>47</sup> the reactions that take place through the type II mechanism are enhanced in D<sub>2</sub>O. Air-equilibrated solutions containing HSA and Ptr in H<sub>2</sub>O and D<sub>2</sub>O were irradiated under otherwise identical conditions (radiation source I), and HSA damage was evaluated.

In particular, NFK has been reported as a typical product of the oxidation of Trp by  $^1\text{O}_2$ .<sup>48</sup> NFK formation was determined in the same way as that explained for the experiment of Figure 9, and the results (inset of Figure 9) showed that NFK formation was faster in D<sub>2</sub>O; however, the difference was not as large as expected for a pure type II mechanism. Therefore, data indicate that the reaction with  $^1\text{O}_2$  is present in our reaction system, but it is not the only contribution for the formation of NFK, thus suggesting that this compound can be also formed via a type I mechanism. In agreement with these results, a similar behavior was observed for the consumption of Trp, measured by fluorescence, in both solvents. Besides, protein damage evaluated by SDS–PAGE showed that the intensity of the HSA band decreased slightly faster in D<sub>2</sub>O than in H<sub>2</sub>O, which suggests that other reactions, apart from Tyr<sub>2</sub> formation, can contribute to the photoinduced oligomerization of HSA (Figure S2).

## CONCLUSIONS

The damage of human serum albumin (HSA) photosensitized by pterin (Ptr) in an aqueous solution under UV-A irradiation was investigated. Ptr is a model compound of oxidized pterins, photosensitizers present in human skin under pathological conditions. The photosensitized process induces chemical changes in the protein in, at least, two amino acids: tryptophan (Trp) and tyrosine (Tyr). On the other hand, the photosensitizer is not consumed in the process. HSA undergoes cross-linking, a process that is not just a dimerization, but a photoinduced oligomerization that yields large protein structures with more than 10 HSA molecules. The bonds between the protein molecules are, at least in part, dimers of Tyr (Tyr<sub>2</sub>), whose concentration increases with irradiation time. The cross-linking does not significantly affect the secondary and tertiary structures of HSA. Trp is also consumed in the photosensitized process, and *N*-formylkynurenine (NFK) was identified as one of its oxidation products. These processes are purely dynamic and are initiated by the triplet excited state of Ptr through production of singlet oxygen and electron transfer oxidation. The results presented in this work allow us to conclude that protein photodamage mediated by endogenous photosensitizers can significantly contribute to the harmful effects of UV-A radiation on the human skin.

## ASSOCIATED CONTENT

### Supporting Information

The Supporting Information is available free of charge on the ACS Publications website at DOI: 10.1021/acs.biochem.6b00420.

Fluorescence spectra and SDS–PAGE analysis of aqueous solutions of HSA irradiated in the presence of Ptr (PDF)

## AUTHOR INFORMATION

### Corresponding Author

\*Address: C. C. 16, Sucursal 4, B1904DPI, La Plata, Argentina. E-mail: ldantola@inifta.unlp.edu.ar. Phone: +54 221 4257430, ext. 153. Fax: +54 221 425464.

### Funding

This work was partially supported by Consejo Nacional de Investigaciones Científicas y Técnicas (CONICET, Grant PIP 0304), Agencia de Promoción Científica y Tecnológica (ANPCyT, Grant PICT 2012-0508), and Universidad Nacional de La Plata (UNLP, Grants X586 and X712). L.O.R. thanks CONICET for a doctoral research fellowship. A.H.T., E.A.R., and M.L.D. are research members of CONICET.

### Notes

The authors declare no competing financial interest.

## ACKNOWLEDGMENTS

The authors deeply acknowledge Dr. Mariana P. Serrano, Dr. Faustino E. Morán Vieyra, and Dr. Claudio D. Borsarelli [INBIONATEC, CITSE-CONICET, Universidad Nacional de Santiago del Estero (UNSE), Santiago del Estero, Argentina] for their crucial contributions to laser-flash photolysis experiments.

## ABBREVIATIONS

BSA, bovine serum albumin; BSA<sup>•+</sup>, bovine serum albumin radical cation; CD, circular dichroism; D<sub>2</sub>O, deuterated water;  $\theta$ , ellipticity; FPLC, fast performance liquid chromatography; FL, fluorescence;  $I_F$ , fluorescence intensity;  $\Phi_F$ , fluorescence quantum yield; HPLC, high-performance liquid chromatography; HSA, human serum albumin;  $R_H$ , hydrodynamic radius; H<sub>2</sub>O<sub>2</sub>, hydrogen peroxide;  $q_{n,p}^{0,V}$ , incident photon flux density;  $I^-$ , iodide;  $t_i$ , irradiation time; LFP, laser-flash photolysis;  $\tau_T$ , lifetime of the triplet excited state of pterin; LS, light scattering; LC, liquid chromatography;  $[\theta]$ , molar ellipticity; TEMED, *N,N,N',N'*-tetramethylethylenediamine; NFK, *N*-formylkynurenine;  $l$ , optical path length; PDA, photodiode array detector; KI, potassium iodide; Ptr, pterin;  $\text{Ptr}^{\bullet-}$ , pterin radical anion;  $k_q^{\text{HSA}}$ , rate constant of quenching of the triplet excited state of Ptr by human serum albumin; ROS, reactive oxygen species;  $I_F/I_F^0$ , relative total fluorescence intensity;  $t_R$ , retention time;  $^1\text{Ptr}^*$ , singlet excited state of pterin;  $^1\text{O}_2$ , singlet oxygen;  $\tau_\Delta$ , singlet oxygen lifetime; SEC, size exclusion chromatography; SDS, sodium dodecyl sulfate; SDS–PAGE, sodium dodecyl sulfate–polyacrylamide gel electrophoresis;  $\text{O}_2^{\bullet-}$ , superoxide anion; H<sub>4</sub>Bip, 5,6,7,8-tetrahydrobiopterin;  $^3\text{Ptr}^*$ , triplet excited state of pterin; Tris, tris(hydroxymethyl)aminomethane; Tyr<sub>2</sub>, tyrosine dimer;  $\alpha$ -MSH,  $\alpha$ -melanocyte-stimulating hormone.



# REFERENCES

- (1) Pfeleiderer, W. (1993) in *Chemistry and Biology of Pteridines and Foliates* (Ayling, J. E., Nair, M. G., and Baugh, C. M., Eds.) pp 1–16, Plenum Press, New York.
- (2) Kappock, T. J., and Caradonna, J. P. (1996) Pterin-dependent aminoacid hydroxylases. *Chem. Rev.* 96, 2659–2756.
- (3) Ziegler, I. (1990) Production of pteridines during hematopoiesis and T-lymphocyte proliferation: potential participation in the control of cytokine signal transmission. *Med. Res. Rev.* 10, 95–114.
- (4) Nichol, C. A., Smith, G. K., and Duch, D. S. (1985) Biosynthesis and metabolism of tetrahydrobiopterin and molybdopterin. *Annu. Rev. Biochem.* 54, 729–764.
- (5) Glassman, S. J. (2011) Vitiligo, reactive oxygen species and T-cells. *Clin. Sci.* 120, 99–120.
- (6) Rokos, H., Beazley, W. D., and Schallreuter, K. U. (2002) Oxidative stress in vitiligo: photo-oxidation of pterins produces H<sub>2</sub>O<sub>2</sub> and pterin-6-carboxylic acid. *Biochem. Biophys. Res. Commun.* 292, 805–811.
- (7) Schallreuter, K. U., Moore, J., Wood, J. M., Beazley, W. D., Peters, E. M. J., Marles, L. K., Behrens-Williams, S. C., Dummer, R., Blau, N., and Thöny, B. J. (2001) Epidermal H<sub>2</sub>O<sub>2</sub> accumulation alters tetrahydrobiopterin (6BH4) recycling in vitiligo: identification of a general mechanism in regulation of all 6BH4-dependent processes? *J. Invest. Dermatol.* 116, 167–174.
- (8) Thomas, A. H., Catalá, A., and Vignoni, M. (2016) Soybean phosphatidylcholine liposomes as model membranes to study lipid peroxidation photoinduced by pterin. *Biochim. Biophys. Acta, Biomembr.* 1858, 139–145.
- (9) Neverov, K. V., Mironov, E. A., Lyudnikova, T. A., Krasnovsky, A. A., Jr., and Kritsky, M. S. (1996) Phosphorescence analysis of the triplet state of pterins in connection with their photoreceptor function in biochemical systems. *Biochemistry (Moscow)* 61, 1149–1155.
- (10) Egorov, S. Yu., Krasnovsky, A. A., Jr., Bashtanov, M. Ye., Mironov, E. A., Ludnikova, T. A., and Kritsky, M. S. (1999) Photosensitization of Singlet Oxygen Formation by Pterins and Flavins. Time-Resolved Studies of Oxygen Phosphorescence under Laser Excitation. *Biochemistry (Moscow)* 64, 1117–1121.
- (11) Lorente, C., and Thomas, A. H. (2006) Photophysics and photochemistry of pterins in aqueous solution. *Acc. Chem. Res.* 39, 395–402.
- (12) Thomas, A. H., Serrano, M. P., Rahal, V., Vicendo, P., Claparols, C., Oliveros, E., and Lorente, C. (2013) Tryptophan oxidation photosensitized by pterin. *Free Radical Biol. Med.* 63, 467–475.
- (13) Castaño, C., Dántola, M. L., Oliveros, E., Thomas, A. H., and Lorente, C. (2013) Oxidation of tyrosine photoinduced by pterin in aqueous solution. *Photochem. Photobiol.* 89, 1448–1455.
- (14) Castaño, C., Oliveros, E., Thomas, A. H., and Lorente, C. (2015) Histidine oxidation photosensitized by pterin: pH dependent mechanism. *J. Photochem. Photobiol., B* 153, 483–489.
- (15) Castaño, C., Lorente, C., Martins-Froment, N., Oliveros, E., and Thomas, A. H. (2014) Degradation of  $\alpha$ -melanocyte-stimulating hormone photosensitized by pterin. *Org. Biomol. Chem.* 12, 3877–3886.
- (16) Thomas, A. H., Lorente, C., Roitman, K., Morales, M. M., and Dántola, M. L. (2013) Photosensitization of bovine serum albumin by pterin: a mechanistic study. *J. Photochem. Photobiol., B* 120, 52–58.
- (17) Thomas, A. H., Zurbano, B. N., Lorente, C., Santos, J., Roman, E. A., and Dántola, M. L. (2014) Chemical changes in bovine serum albumin photoinduced by pterin. *J. Photochem. Photobiol., B* 141, 262–268.
- (18) Dántola, M. L., Gojanovich, A. D., and Thomas, A. H. (2012) Inactivation of tyrosinase photoinduced by pterin. *Biochem. Biophys. Res. Commun.* 424, 568–572.
- (19) Dántola, M. L., Zurbano, B. N., and Thomas, A. H. (2015) Photoinactivation of tyrosinase sensitized by folic acid photoproducts. *J. Photochem. Photobiol., B* 149, 172–179.
- (20) Peters, T. (1996) *All about Albumin: Biochemistry, Genetic and Medical Applications*, p 432, Academic Press, San Diego.
- (21) He, X. M., and Carter, D. C. (1992) Atomic structure and chemistry of human serum albumin. *Nature* 358, 209–215.
- (22) Dockal, M., Chang, M., Carter, D. C., and Ruker, F. (2000) Five recombinant fragments of human serum albumin- Tools for the characterization of the warfarin binding site. *Protein Sci.* 9, 1455–1465.
- (23) Hagag, N., Birnbaum, E. R., and Darnall, D. W. (1983) Resonance Energy Transfer between cysteine-34, tryptophan-214, and tyrosine-411 of human serum albumin. *Biochemistry* 22, 2420–2427.
- (24) Katz, J., Bonorris, G., and Sellars, A. L. (1970) Extravascular albumin in human tissues. *Clin. Sci.* 39, 725–729.
- (25) Hasse, S., Kothari, S., Rokos, H., Kauser, S., Schürer, N. Y., and Schallreuter, K. U. (2005) In vivo and in vitro evidence for autocrine DCoH/HNF-1a transcription of albumin in the human epidermis. *Exp. Dermatol.* 14, 182–187.
- (26) Rokos, H., Moore, J., Hasse, S., Gillbro, J., Wood, J. M., and Schallreuter, K. U. (2004) In vivo fluorescence excitation spectroscopy and in vivo Fourier-transform Raman spectroscopy in human skin: evidence of H<sub>2</sub>O<sub>2</sub> oxidation of epidermal albumin in patients with vitiligo. *J. Raman Spectrosc.* 35, 125–130.
- (27) Monópoli, V. D., Thomas, A. H., and Capparelli, A. L. (2000) Kinetics and equilibrium study of nickel(II) complexation by pterin and 6-carboxypterin. *Int. J. Chem. Kinet.* 32, 231–237.
- (28) Alarcón, E., Edwards, A. M., Aspée, A., Borsarelli, C. D., and Lissi, E. A. (2009) Photophysics and photochemistry of rose bengal bound to human serum albumin. *Photochem. Photobiol. Sci.* 8, 933–943.
- (29) Braslavsky, S. E. (2007) Glossary of terms used in photochemistry, 3rd edition (IUPAC Recommendations 2006). *Pure Appl. Chem.* 79, 293–465.
- (30) Kuhn, H. J., Braslavsky, S. E., and Schmidt, R. (2004) Chemical actinometry (IUPAC technical report). *Pure Appl. Chem.* 76, 2105–2146.
- (31) Serrano, M. P., Vignoni, M., Dántola, M. L., Oliveros, E., Lorente, C., and Thomas, A. H. (2011) Emission properties of dihydropterins in aqueous solutions. *Phys. Chem. Chem. Phys.* 13, 7419–7425.
- (32) Kanwar, R., and Balasubramanian, D. (2000) Structural studies on some dityrosine-cross linked globular proteins: stability is weakened, but activity is not abolished. *Biochemistry* 39, 14976–14983.
- (33) Harms, G. S., Pauls, S. W., Hedstrom, J. F., and Johnson, C. K. (1997) Fluorescence and rotational dynamics of dityrosine. *J. Fluoresc.* 7, 283–292.
- (34) Mahmoud, S. F., and Bialkowski, S. E. (1995) Laser-excited fluorescence of Dityrosine. *Appl. Spectrosc.* 49, 1669–1676.
- (35) Lakowicz, J. R. (2006) *Principles of Fluorescence Spectroscopy*, Chapter 3, Springer, New York.
- (36) Fukunaga, Y., Katsuragi, Y., Izumi, T., and Sakiyama, F. (1982) Fluorescence characteristics of kynurenine and N'-formylkynurenine. Their use as reporters of the environment of tryptophan 62 in Hen Egg-white lysozyme. *J. Biochem.* 92, 129–141.
- (37) De Wolf, F. A., and Brett, G. M. (2000) Ligand binding proteins: their potential for application in systems for controlled delivery and uptake of ligands. *Pharmacol. Rev.* 52, 200–236.
- (38) Thomas, A. H., Lorente, C., Capparelli, A. L., Pokhrel, M. R., Braun, A. M., and Oliveros, E. (2002) Fluorescence of pterin, 6-formylpterin, 6-carboxypterin and folic acid in aqueous solutions: pH effects. *Photochem. Photobiol. Sci.* 1, 421–426.
- (39) Chahidi, C., Aubailly, M., Momzikoff, M., Bazin, M., and Santus, R. (1981) Photophysical and Photosensitizing properties of 2-amino-4 Pteridinone: a natural pigment. *Photochem. Photobiol.* 33, 641–649.
- (40) Petroselli, G., Dántola, M. L., Cabrerizo, F. M., Capparelli, A. L., Lorente, C., Oliveros, E., and Thomas, A. H. (2008) Oxidation of 2'-Deoxyguanosine 5'-Monophosphate Photoinduced by Pterin: Type I versus Type II Mechanism. *J. Am. Chem. Soc.* 130, 3001–3011.
- (41) Serrano, M. P., Lorente, C., Borsarelli, C. D., and Thomas, A. H. (2015) Unraveling the Degradation Mechanism of Purine Nucleotides Photosensitized by Pterins: The Role of Charge-Transfer Steps. *ChemPhysChem* 16, 2244–2252.

- (42) Kritsky, M. S., Lyudnikova, T. A., Mironov, E. A., and Moskaleva, I. V. J. (1997) The UV radiation-driven reduction of pterins in aqueous solution. *J. Photochem. Photobiol., B* 39, 43–48.
- (43) Denofrio, M. P., Ogilby, P. R., Thomas, A. H., and Lorente, C. (2014) Selective quenching of triplet excited states of pteridines. *Photochem. Photobiol. Sci.* 13, 1058–1065.
- (44) Pattison, D. I., Rahmanto, A. S., and Davies, M. J. (2012) Photo-oxidation of proteins. *Photochem. Photobiol. Sci.* 11, 38–53.
- (45) Malencik, D. A., and Anderson, S. R. (2003) Dityrosine as a product of oxidative stress and fluorescent probe. *Amino Acids* 25, 233–247.
- (46) Spikes, J. D., Shen, H. R., Kopečková, P., and Kopeček, J. (1999) Photodynamic crosslinking of proteins. III. Kinetics of the FMN- and rose bengal-sensitized photooxidation and intermolecular crosslinking of model tyrosine-containing N-(2-hydroxypropyl)methacrylamide copolymers. *Photochem. Photobiol.* 70, 130–137.
- (47) Foote, C. S., and Clennan, E. L. (1995) Properties and reaction of singlet dioxygen. In *Active Oxygen in Chemistry* (Foote, C. S., Valentine, J. S., Greenberg, A., and Liebman, J. F., Eds.) Vol. 2, p 104, Chapman & Hall, New York.
- (48) Ronsein, G. E., Oliveira, M. C. B., Miyamoto, S., Medeiros, M. H. G., and Di Mascio, P. (2008) Tryptophan oxidation by singlet molecular oxygen [ $O_2 (^1\Delta_g)$ ]: Mechanistic studies using  $^{18}O$ -labeled hydroperoxides, mass spectrometry, and light emission measurements. *Chem. Res. Toxicol.* 21, 1271–1283.